

Mid-infrared interferometry on spectral lines:
II. Continuum (dust) emission around IRC +10216 and VY CMa

J. D. Monnier¹, W. C. Danchi², D. S. Hale, E. A. Lipman³, P. G. Tuthill⁴, and C. H. Townes
Space Sciences Laboratory, University of California, Berkeley, Berkeley, CA 94720-7450

ABSTRACT

The U. C. Berkeley Infrared Spatial Interferometer has measured the mid-infrared visibilities of the carbon star IRC +10216 and the red supergiant VY CMa. The dust shells around these sources have been previously shown to be time-variable, and these new data are used to probe the evolution of the dust shells on a decade time-scale, complementing contemporaneous studies at other wavelengths. Self-consistent, spherically-symmetric models at maximum and minimum light both show the inner radius of the IRC +10216 dust shell to be much larger (150 mas) than that expected from the dust condensation temperature, implying that dust production has slowed or stopped in recent years. Apparently, dust does not form every pulsational cycle (638 days), and these mid-infrared results are consistent with recent near-IR imaging which indicates little or no new dust production in the last three years (Tuthill *et al.* 2000). Spherically symmetric models failed to fit recent VY CMa data, implying that emission from the inner dust shell is highly asymmetric and/or time-variable.

Subject headings: instrumentation: interferometers, techniques: interferometric, stars: AGB and post-AGB, stars: circumstellar matter, stars: winds

¹Current Address: Smithsonian Astrophysical Observatory MS#42, 60 Garden Street, Cambridge, MA, 02138

²Current Address: NASA Goddard Space Flight Center, Infrared Astrophysics, Code 685, Greenbelt, MD 20771

³Current Address: Laboratory of Chemical Physics, Building 5, Room 114, National Institutes of Health, Bethesda, MD, 20892-0520

⁴Current Address: Chatterton Astronomy Dept, School of Physics, University of Sydney, NSW 2006, Australia

1. Introduction

Long-baseline infrared interferometry has been effective in characterizing the *general* properties of dust shells around late-type stars (e.g., Danchi et al. 1994) for some years, establishing that dust shells can be produced both continuously (dust shell inner radii $\sim 2\text{--}3 R_\star$) and episodically (dust shell inner radii $\gg 1 R_\star$) (e.g., Dyck et al. 1984; Danchi et al. 1994; Bester et al. 1996). However, recent studies have also shown that the dust shells around certain stars can change significantly in the span of a few years (e.g., Bester et al. 1996; Lopez et al. 1997; Haniff & Buscher 1998), challenging our understanding of the physics responsible for the dust production and the mass-loss in general.

In order to understand what conditions precipitate the formation of stable, long-term dust and molecular envelopes, regular observations of the dust shells around a number of sources are required. Monitoring the dust as it forms, is driven away by radiation pressure, and ultimately replenished by fresh material, promises to elucidate the intimate relationship between stellar pulsations and dust production. High-resolution observations of the inner region of these dust shells are easiest to interpret in the mid-infrared because of high dust opacities and scattered nebulosity encountered in the visible and near-infrared. In addition, interferometric observations allow for detection of global asymmetries in the dust emission, but there have been few confirmed reports of mid-infrared asymmetries around AGB stars (e.g., McCarthy 1979), mostly because of limited spatial resolution. Asymmetries in the mass-loss flow are readily apparent in images of planetary nebulae (e.g., Sahai 1998), yet it is still not clear how much asymmetry begins during the AGB stage or afterwards.

In this paper, we present visibility data from the Infrared Spatial Interferometer (ISI) for carbon star IRC +10216 and red supergiant VY CMa. It has been nearly a decade since these stars have been observed at similar spatial resolution (Danchi et al. 1994), and these new data uniquely probe the temporal evolution of the dust shells over this time span. In addition, wide position angle coverage was obtained for observations of VY CMa, allowing the symmetry of its inner dust shell to be directly measured. The next paper in this series (Monnier *et al.* 2000) utilizes the new dust shell models developed herein to interpret mid-infrared absorption lines from polyatomic molecules forming in the dusty outflows.

2. Methodologies

A brief summary of the observing and modeling methodologies for the Infrared Spatial Interferometer will be presented in this section; further information can be found in previous papers and publications, most notably Danchi *et al.* (1994) and Hale *et al.* (2000).

2.1. Observations

The Infrared Spatial Interferometer (ISI) is a two-element, heterodyne stellar interferometer operating at discrete wavelengths in the 9–12 μm range and is located on Mt. Wilson, CA. The telescopes are each mounted within a movable semi-trailer and together can currently operate at baselines ranging from 4 to 56 m. Detailed descriptions of the apparatus and recent upgrades can be found in Lipman (1998) and Hale *et al.* (2000). System calibration was maintained by observations of partially resolved K giant stars α Tau and α Boo which have no known circumstellar dust. This approach has proven to be successful at calibrating the overall visibility data to a precision of about $\pm 5\%$.

By observing a target star throughout the night, visibility data are obtained at a variety of baselines, owing to the changing projection of the telescope separation vector as the star moves across the sky. Data taken on various nights and with different telescope spacings are collated and uncertainty estimates produced by inspecting the internal scatter of the measurements at similar spatial frequencies. The sparse Fourier coverage afforded by the ISI’s single baseline and concomitant lack of Fourier phase (or closure phase) measurements severely constrains the types of analyses that can be pursued. Thus aperture synthesis techniques are of limited utility, and interpretation of the data relies largely on radiative transfer calculations of simple dust shell models.

2.2. Radiative Transfer Modeling

Physical parameters of dust shells around evolved stars can be obtained through modeling, i.e. directly fitting the visibility data. This allows additional observations, such as spectrophotometry or interferometric work at other wavelengths, to be included as constraints on the modeling. The radiative transfer modeling code used for this purpose is based on the work of Wolfire & Cassinelli (1986) and assumes the dust distribution to be spherically symmetric (see Danchi *et al.* [1994] for a detailed description). Starting with the optical properties and density distribution of the dust grains, this code calculates the equilibrium temperature of the dust shell as a function of the distance from the star, whose spectrum is assumed to be a blackbody. Subsequent radiative transfer calculations at 67 separate wavelengths allow the wavelength-dependent visibility curves, the broadband spectral energy distribution, and the mid-infrared spectrum all to be computed for comparison with observations. The 8–12 μm band is densely sampled, and has been useful for comparing with UKIRT spectrophotometric monitoring (Monnier, Geballe, & Danchi 1998).

The model simulates a star of radius R_\star and temperature T_{eff} situated at the center of the dust shell. Because of high temperatures preventing dust condensation, there is a dust-free spherical region extending from the photosphere to the dust shell inner radius, R_{dust} . For the simple models under consideration here, the density distribution of dust is constrained to follow a power law from R_{dust} to R_{outer} , at which point the dust density is assumed to drop to zero again. Typically (and in all cases for this paper), *uniform outflow* is assumed, implying the dust density falls off like

$\rho \propto R^{-2}$, and R_{outer} is taken to be large enough to contain all significant thermal emission (in the mid-IR) of the dust. The overall density of the dust shell is parameterized by the optical depth τ at $11.15 \mu\text{m}$ along a line-of-sight connecting the observer with the star.

The code treats a distribution of dust sizes by calculating the dust temperature as a function of grain size and dust type (e.g. dirty silicates, amorphous carbon, graphite), using the Mathis, Rumpl, & Nordsieck (1977) grain size distribution, where the grain size a spans $0.01 \mu\text{m} < a < 0.25 \mu\text{m}$ with number density $n \propto a^{-3.5}$. Dust opacities were calculated from the optical constants assuming spheroidal Mie scattering using a method developed by Toon & Ackerman (1981). The warm silicate dust constants from Ossenkopf *et al.* (1992) and the amorphous carbon (AC) dust constants from Rouleau & Martin (1991) were used for modeling oxygen-rich and carbon-rich dust shells respectively.

3. ISI Results and Modeling of Dust Shells

New ISI visibility data for IRC +10216 and VY CMa presented here, along with recent mid-infrared spectra, are used to constrain radiative transfer models of the circumstellar dust shells. For any given source, it is difficult or impossible to fit the vast array of multi-wavelength data available using a simple model (see Monnier *et al.* [1997] and Groenewegen [1997] for recent attempts). This difficulty is largely due to the overly-simple nature of the models (e.g., spherical symmetry), unknown dust properties (e.g., grain size distribution, effects of large grains), and the lack of coeval data for these pulsating stars. Because we are partly concerned with the dust shell as a mid-IR background continuum source for molecular absorption, the modeling found herein is focused on reproducing the observed mid-infrared properties in Fall 1998 when molecular line data was collected (see Monnier *et al.* 2000). Hence, the data and modeling results are presented for Fall 1998 separate from other epochs. In order to implicitly include observations at other wavelengths and from other epochs, some choices of model parameters have been guided by the results of previous, more detailed modeling work, when available.

3.1. IRC +10216

3.1.1. Introduction

The long-period variable star IRC +10216 was discovered by Neugebauer & Leighton (1969) during the $2.2 \mu\text{m}$ sky survey, and its optical counterpart was shown to be extended and asymmetric (Becklin *et al.* 1969). It was soon recognized to be an evolved giant star surrounded by an opaque envelope of dust, whose intense thermal emission makes it one of the brightest mid-infrared sources outside the solar system.

Because of its high infrared brightness and the large number of molecules found in its dense

outflow, IRC +10216 has become one of the most studied objects in the galaxy; the Astrophysics Data System lists nearly 1000 papers associated with this star. In particular, the large angular size of the dust shell, first established through lunar occultation work (Toombs et al. 1972), has made IRC +10216 a favorite target of interferometrists (see below).

Spectral observations have revealed a carbon-rich envelope (Herbig & Zappala 1970) and subsequent workers have identified over 50 different molecular species in the circumstellar environment (Glassgold 1998), most in radio and millimeter transitions. IRC +10216 has become prototypical of extreme evolved carbon stars, a rare stellar specimen representing a brief, but important, phase of heavy mass-loss in the late stages of stellar evolution. The mass-loss rate has been estimated through observations of J=2-1 line of CO and from mid-infrared interferometric observations to be $\sim 3 \times 10^{-5} M_{\odot} yr^{-1}$ (Knapp et al. 1982; Danchi et al. 1994), assuming a distance of 135 pc (Groenewegen 1997). Recently, its inner dust shell has been imaged and shown to be highly inhomogeneous and asymmetric (Weigelt et al. 1998; Haniff & Buscher 1998; Tuthill, Monnier & Danchi 1998; Skinner, Meixner & Bobrowsky 1998; Monnier 1999; Tuthill et al. 2000). Observations of the outer envelope (e.g., Bieging & Tafalla 1993) indicate a more or less spherically symmetric outflow, and so it has been suggested that IRC +10216 is presently undergoing a transformation from a (spherically symmetric) red giant star to a (asymmetric) planetary nebula. If so, we are witnessing an extremely short-lived phase and high spatial resolution observations are critical to understanding the complicated processes at play.

While the inner region of the dust shell has already been shown to be high clumpy (see references above) in the near-infrared and visible, the mid-infrared emission is expected to be more symmetrical because of enhanced emission from cooler dust grains farther out in the flow, which contribute substantially to the total mid-infrared flux. However, data from the single baseline of the ISI cannot untangle complicated effects due to deviations from spherical symmetry. A number of other authors have found that spherically symmetric models of the dust shell around IRC +10216 can fit most of the spectral and imaging data, at least redward of $\sim 2 \mu\text{m}$ (e.g., Ivezić & Elitzur 1996; Groenewegen 1997). At shorter wavelengths, scattering in the inhomogeneous and clumpy inner dust shell dominate the appearance (Haniff & Buscher 1998; Skinner, Meixner & Bobrowsky 1998) and spherically symmetric models begin to fail. While recognizing these uncertainties, in this section we develop a spherically symmetric model of the dust shell around IRC +10216.

3.1.2. Data from Fall 1998

The visibility curve of IRC +10216 at $11.15 \mu\text{m}$ was measured on 1998 Nov 18 (UT) with a 4-meter, East-West baseline. Earth rotation foreshortened the baseline and allowed a range of spatial frequencies to be used. Details concerning data reduction and calibration can be found in Hale *et al.* (2000) and references therein.

Table 1 and figure 1 show the visibility data for IRC +10216 calibrated using α Tau, approx-

imately a point source at the resolution of this experiment. The ISI detects only radiation within the telescope primary beam, FWHM \sim 1.8'' for the 1.65 m apertures. This significantly modifies the observed visibility curves from those obtainable using an interferometer with smaller aperture telescopes. Active image stabilization could not be used for obscured sources such as IRC +10216 and allow the outer parts of the nebula to be detected as well. This effect was included in the modeling described below by multiplying the model emission profiles by an appropriately-sized primary beam pattern centered on the central star. The Gaussian FWHM used is reported in the parameter tables for all models. Furthermore, the decorrelation resulting from independent guiding errors in each telescope is appropriately calibrated by observing the calibrator source under similar observing conditions.

3.1.3. *The dust model*

The best-fitting model parameters for a uniform outflow dust shell appear in table 2, and were discussed in §2.2. The new ISI visibility data from November 1998 and a mid-infrared spectrum taken at pulsational phase 0.65 (Monnier *et al.* 1998) were used to constrain the model fitting parameters. This spectrum was chosen to closely coincide with the pulsational phase of IRC +10216 during the observation ($\phi_{\text{IR}} \sim 0.76$). The data and model fits can be found in figures 1 & 2 and are quite satisfactory, considering the simplicity of the dust density distribution. Note that the SiC feature near 11.3 μm was not included in the optical constants, resulting in a systematic misfit in this spectral region.

The inner radius (150 mas) and mid-IR optical depth agree quite well (within 10%) with the dust shell parameters in Groenewegen (1997), who recently modelled the source at maximum light. However, this inner radius is significantly larger than that deduced by models based on data taken approximately a decade ago, ~ 75 mas deduced from earlier epochs of ISI data (Danchi *et al.* 1994) and 95 ± 10 mas from near-infrared data (Ridgway & Keady 1988). At 150 mas away from IRC +10216 near minimum light, the dust temperature is only about 860K, significantly below the condensation temperature (~ 1400 K). This can be explained if the dust was initially created 5-10 years ago and has been flowing outward since that time. This is also consistent with recent near-IR images of the inner dust zone, which show a clumpy outwardly expanding dusty environment with no obvious new dust production within the last 3 years (Haniff & Buscher 1998, Weigelt *et al.* 1998, Tuthill, Monnier & Danchi 1998, Monnier 1999, Tuthill *et al.* 2000). This dust shell model will be used for subsequent modeling of molecular absorption around IRC +10216 (Monnier *et al.* 2000).

Table 1. IRC +10216 Visibility Data from November 1998 ($\lambda=11.15 \mu\text{m}$)

Spatial Frequency (10^5 rad^{-1})	Position Angle ($^\circ$)	Visibility	Visibility Uncertainty
2.19	110.5	0.314	0.017
2.36	108.2	0.310	0.017
2.64	104.8	0.237	0.017
2.78	103.2	0.211	0.009
2.91	101.8	0.180	0.024
3.06	100.3	0.181	0.013
3.23	98.4	0.158	0.012
3.36	96.8	0.141	0.007
3.53	94.4	0.128	0.008
3.61	91.4	0.098	0.020

Table 2. IRC +10216 Model Parameters for Uniform Outflow Fit (November 1998 data)

Parameter	Value	Comments
Distance (pc)	135	From Groenewegen (1997)
T_{eff} (K)	2000	From Groenewegen (1997)
Stellar Radius (mas)	22.0	
Luminosity (L_{\odot})	5892	To fit mid-IR spectrum
Dust Type	Amorphous Carbon (type A-C)	From Rouleau & Martin (1991)
Dust Size Distribution	$n \propto a^{-3.5}$	From Mathis, Rumpl, & Nordsieck (1977)
R_{dust} (mas)	150	Inner radius of dust, chosen to fit mid-IR visibility
τ at $11.15\mu\text{m}$	0.66	Optical Depth, chosen to fit mid-IR spectral slope
Effective Primary Beamwidth ($''$)	3.00	

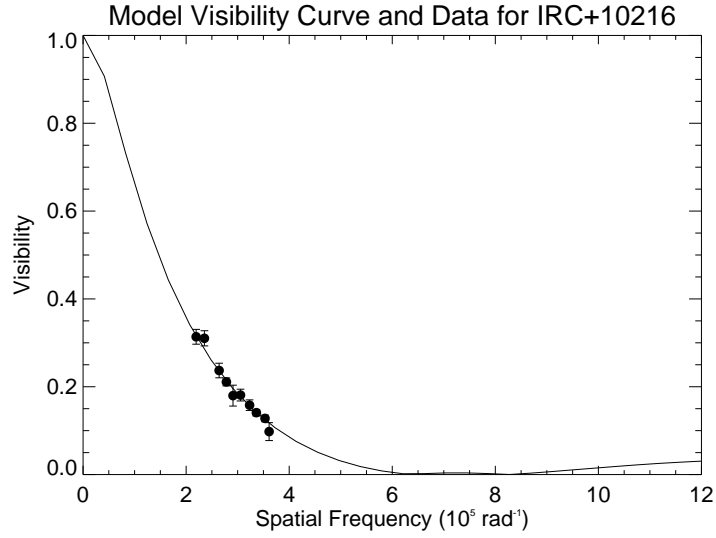


Fig. 1.— The new mid-infrared visibility data for IRC +10216 in November 1998 and model results are shown. The solid line is the model visibility curve based on the parameters in Table 2, assuming a primary beam of $3''$.

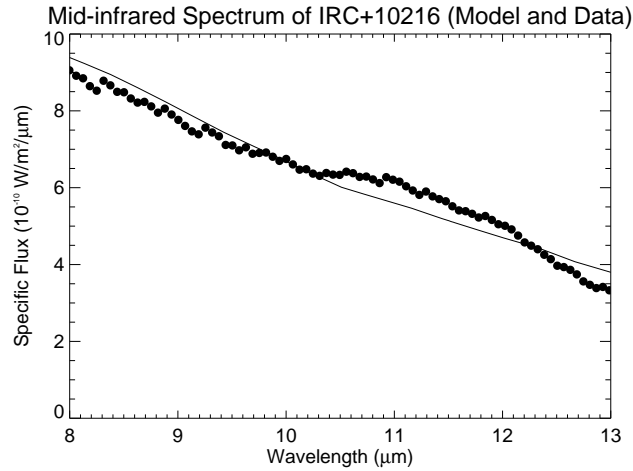


Fig. 2.— The mid-infrared spectrum of IRC +10216 taken on 1995 March 17 at a phase similar to that of IRC +10216 during 1998 November interferometric observations (Monnier *et al.* 1998). The solid line is the model spectrum based on the parameters in Table 2. The dust mixture used did not contain SiC, hence the spectral feature near $11.3 \mu\text{m}$ was not fitted here.

Table 3. IRC +10216 Visibility Data from November 1997 and April 1999 ($\lambda=11.15 \mu\text{m}$)

Spatial Frequency (10^5 rad^{-1})	Position Angle ($^\circ$)	Visibility	Visibility Uncertainty	Date of Observation (UT)
1.58	64.7	0.402	0.020	1999 Apr 26-27
1.73	67.6	0.368	0.018	1999 Apr 26-27
1.87	69.4	0.355	0.019	1999 Apr 26-27
2.03	72.3	0.307	0.010	1999 Apr 26-27
2.64	79.6	0.205	0.021	1999 Apr 26
2.74	80.2	0.173	0.018	1999 Apr 26
3.34	87.1	0.112	0.011	1999 Apr 27
6.7	326	0.0000	0.0036	1997 Nov 21
7.3	317	0.0056	0.0033	1997 Nov 21
8.6	299	0.0104	0.0009	1997 Nov 23
11.0	347	0.0125	0.0007	1997 Nov 01
11.4	338	0.0050	0.0023	1997 Nov 01
11.9	332	0.0054	0.0009	1997 Nov 01

3.1.4. Data from other epochs

Special care was made to model the dust shell of IRC +10216 during Fall 1998 because spectral line data were also collected during this epoch (Monnier *et al.* 2000). However, additional data were collected on 16 m and 9 m baselines in early November 1997 and on a 4 m baseline in April 1999. The (IR) pulsational phases for these two observations were ~ 0.18 and 0.01 respectively, and the data for these observations can be found in table 3.

Since both sets were taken near maximum light, the stellar luminosity ($15000 L_{\odot}$) and effective temperature (2000 K) from Groenewegen (1997) were used for modeling the stellar output. However, the dust shell model developed to fit the Fall 1998 data was completely unmodified (see table 2 for parameters). The additional luminosity decreased visibilities somewhat from Fall 1998 model values, and the comparison to the Spring 1999 data is quite favorable (see figure 3). This means that the differences in the mid-infrared visibilities can be completely explained by the varying luminosity of the underlying star, without invoking new dust production or significant dust shell evolution between epochs. The disagreement at the longest baseline may be due to inhomogeneities and asymmetries in the dust shell, reflecting very high resolution structure not incorporated in spherically symmetric models.

3.2. VY CMa

3.2.1. Introduction

VY CMa (spectral type M5eIbp) is a very unusual star, displaying intense radio maser emission from a variety of molecules, strong dust emission in the mid-infrared, high polarization in the near-infrared, and large amplitude variability in the visible. Many properties of VY CMa were recently reviewed in Monnier *et al.* (1999a), which included new near-IR imagery of its complicated circumstellar environment.

Using a distance estimate of 1.5 kpc based on work by Lada & Reid (1978) and observations of maser proper motions (Marvel 1996; Richards, Yates, & Cohen 1998), Monnier *et al.* (1999a) estimated the true, obscuration-corrected luminosity to be $L_{\star} \approx 2 \times 10^5 L_{\odot}$. The high luminosity, coupled with an extremely low effective temperature $T_{\star} \approx 2800$ K (Le Sidaner & Le Bertre 1996), suggests VY CMa is a massive star ($M_{\star} \approx 25 M_{\odot}$) on the verge of exploding as a supernova (within $\sim 10^4$ years, Brunish & Truran 1982). Another sign of impending cataclysm is the extensive mass being lost by VY CMa into an optically thick circumstellar envelope. The mass loss rate for this star has been estimated using a variety of techniques (summarized in Danchi *et al.* [1994]), yielding a most probable value of $\dot{M} \approx 2 \times 10^{-4} M_{\odot} \text{ yr}^{-1}$.

Previous observations of the circumstellar envelope at a variety of wavelengths have shown evidence of significant asymmetries. Maser emission of SiO, H₂O, and OH show spatial and redshift distributions not consistent with simple outflow geometries (e.g. Benson & Mutel 1979; Marvel

1996; Richards, Yates, & Cohen 1998). In addition, optical observers have noted VY CMa’s peculiar one-sided nebulosity for most of this century (Worley 1972; Herbig 1972). Indeed, recent visible images from the Hubble Space Telescope (Kastner & Weintraub 1998, Smith et al. 1999) and near-IR adaptive optics observations (Monnier et al. 1999a) show a one-sided reflection nebula, with a complicated arrangement of scattering features. High values of near-infrared linear polarization have been observed, resulting from small-scale asymmetries close to the star itself (Monnier et al. 1999a). McCarthy (1979) reported asymmetry in the mid-infrared emission of the dust shell, interpreting this as evidence for thermal emission from a disk-like structure. Another important observational fact is that VY CMa is an irregular variable star showing 1-3 mag optical variation on the time scale of ~ 2000 days (Marvel 1996). Other observations testifying to the dynamic nature of this source are recent changes in the direction of the near-infrared polarization (Maihara et al. 1976) and shape of the mid-infrared spectrum (Monnier, Geballe, & Danchi 1998, 1999)

3.2.2. Data from Fall 1998

The $11.15\ \mu\text{m}$ visibility curve of VY CMa was measured over a two-day period, from 1998 November 18 to 1998 November 19 (UT) with the ISI in its 4-meter, East-West baseline configuration. Details concerning data reduction and calibration are identical to those for IRC +10216.

3.2.3. The dust model

Despite the evidence for asymmetries in the inner dust shell, spherical symmetry was adopted for modeling the average properties of the mid-IR emission. The best-fitting model parameters for a uniform outflow dust shell appear in table 5. The new ISI visibility data from November 1998 and a mid-infrared spectrum (Monnier *et al.* 1998) were used to constrain the model fitting parameters. VY CMa does not have a well-defined pulsational period and because we have no good estimate of its flux level in November 1998, a mid-IR spectrum of intermediate brightness (1995 Mar 17) was used. The data and model fits can be found in figures 4 & 5 and are in good agreement. Note that the model silicate feature near $9.7\ \mu\text{m}$ appears with a decreased peak due to self-absorption, although not as flat as the observed spectrum.

The inner radius (50 mas) and mid-IR optical depth agree well with previous modeling based on mid-infrared interferometric measurements (Danchi et al. 1994). According to the current model, the dust temperature at this inner radius is about 1300 K, which is roughly the expected condensation temperature for silicate dust grains. Note that this inner radius is in striking disagreement with the modeling results of Le Sidaner (1996) whose fitting procedure only considered the broadband spectral energy distribution (SED). While their best fitting models indicate a dust shell inner radius of 120 mas, the authors noted that the VY CMa results were “certainly the least satisfactory in [their] work.” This illustrates the importance of high angular resolution observations

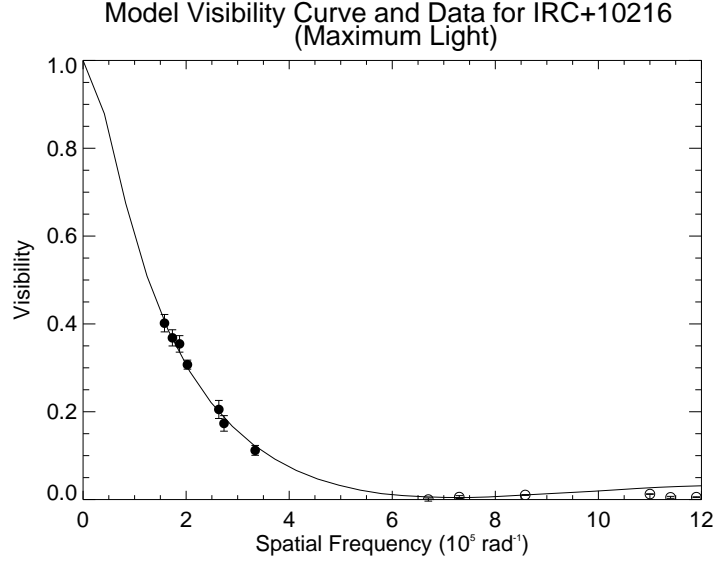


Fig. 3.— Mid-infrared visibility data for IRC +10216 taken on 1999 Apr 26-27 (UT) (filled circles, $\phi_{\text{IR}} = 0.01$) and 1997 Nov 1-23 (UT) (open circles, $\phi_{\text{IR}} = 0.16$ -0.19). The model visibility curve is shown as a solid line assuming a $3''$ primary beam.

Table 4. VY CMa Visibility Data from November 1998 ($\lambda=11.15 \mu\text{m}$)

Spatial Frequency (10^5 rad^{-1})	Position Angle ($^\circ$)	Visibility	Visibility Uncertainty
2.51	62.5	0.49	0.10
2.63	65.3	0.46	0.06
2.79	68.2	0.42	0.04
2.93	71.7	0.41	0.05
3.08	74.9	0.33	0.04
3.23	77.6	0.36	0.03

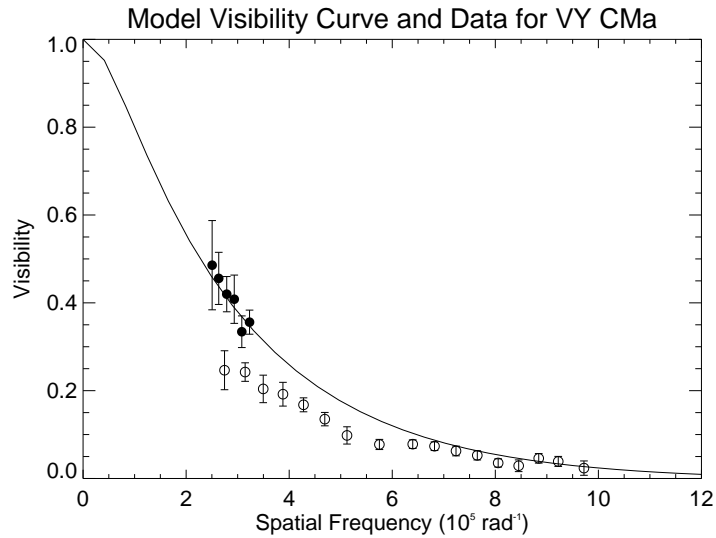


Fig. 4.— The mid-infrared visibility data for VY CMa and the model results are shown. The model visibility curve (solid line) is based on data obtained in Fall 1998 (solid circles), while Fall 1997 data are represented by open circles (see §3.2.4 for discussion of discrepancy). See Table 5 for model parameters.

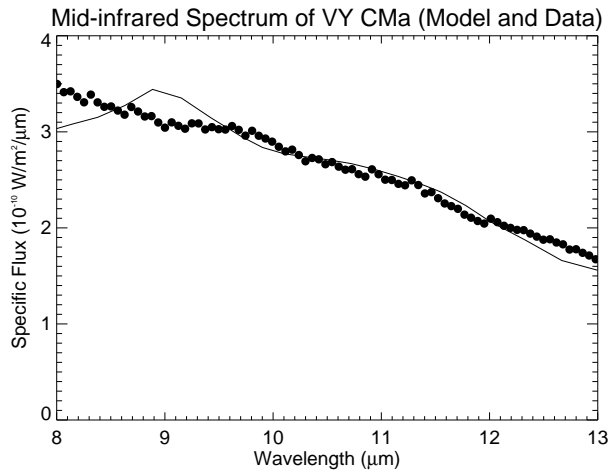


Fig. 5.— A typical mid-infrared spectrum of VY CMa (from 1995 March 17; Monnier *et al.* [1998]) and the model fit (solid line). See Table 5 for more details on model parameters.

for properly constraining radiative transfer models.

Because the dust shell around this star appears asymmetric on all observed scales (10-10000 AU; e.g., Monnier *et al.* 1999a), this simple spherically symmetric model should be considered a rough approximation of the true dust shell; we attempt here only to represent some kind of “average” dust density distribution. This has proven adequate for interpreting the spectral line results discussed in the next paper of this series (Monnier *et al.* 2000).

3.2.4. Data from other epochs

VY CMa was also observed by the ISI in October 1997 with a 16m baseline. This configuration allowed the visibility to be sampled at projected baselines from about 3 to 10 meters. These data have been plotted along with Fall 1998 data on figure 4 (numerical values can be found in table 6). Significant differences in the short baseline data at the two epochs can be seen (at $\sim 3 \times 10^5 \text{ rad}^{-1}$), plausibly arising from changes in the dust shell between observations, deviations from circular symmetry, or anomalous miscalibration at low elevation. These possibilities will be discussed in turn.

Near-constancy in the near-infrared brightness distribution from January 1997 to January 1999 (Monnier *et al.* 1999a; recent unpublished data) suggests that no significant changes in the dust shell occurred between the ISI observations of October 1997 and November 1998. Interestingly, the short baseline observations in 1997 and 1998 were sampling nearly orthogonal position angles on the sky (see tables 4 & 6, where angles are measured in degrees East of North). Hence, the visibility differences could be due to dust shell asymmetry (e.g., NW-SE elongation). Unfortunately, VY CMa was at unavoidably low sky elevations during short baseline observations on the 16m baseline. While accurate calibrations were generally attainable in such cases, it is possible that anomalous atmospheric conditions at low elevation could have caused the lower visibility observed, mimicking the aforementioned dust shell asymmetry.

An asymmetric dust distribution is suggested by high resolution, near-infrared and visible imaging of VY CMa’s circumstellar environment. A NW-SE elongation direction roughly coincides with the “equatorial plane” of enhanced mass-loss inferred to exist from the morphology of the reflection nebula (Kastner & Weintraub 1998, Monnier *et al.* 1999a), but is not in agreement with an earlier mid-IR measurement reported by McCarthy *et al.* (1980). Diffraction-limited imaging with 8 m-class telescopes in the mid-infrared should resolve these ambiguities in interpretation.

4. Conclusions

We have presented new visibility data and models of the dust shells for the carbon star IRC +10216 and the red supergiant VY CMa. Spherically symmetric, uniform outflow models

were adequate to fit most of the mid-infrared properties of these sources. We find that the inner radius of the IRC +10216 dust shell is much larger than that expected if dust was continuously condensing out of the gas; this is in contrast to earlier epochs which showed material much closer to the star. From this, we conclude that little new dust has been produced around IRC +10216 during the last 5-10 years. However, the dust shell around VY CMa appears very similar to that first observed by the ISI around 1990, implying continuous production of dust over the intervening years. These new data have enhanced position angle coverage, yielding evidence for a marked asymmetry of the inner dust shell of VY CMa, although the data are also consistent with pure time evolution. The dust envelopes around these stars are sufficiently large that diffraction-limited observations using a mid-infrared instrument on an 8 m-class telescope should resolve possible asymmetries and vastly improve our understanding of these dust shells, as well as the physical causes for the development of mass-loss asymmetry during the final stages of stellar evolution.

This work is a part of a long-standing interferometry program at U.C. Berkeley, supported by the National Science Foundation (Grant AST-9221105, AST-9321289, and AST-9731625) , the Office of Naval Research (OCNR N00014-89-J-1583), and NASA.

REFERENCES

- Becklin, E. E., Frogel, J. A., Hyland, A. R., Kristian, J. & Neugebauer, G. 1969, *ApJ*, 158, L133
- Benson, J. M. & Mutel, R. L. 1979, *ApJ*, 233, 119
- Bester, M., Danchi, W. C., Hale, D., Townes, C. H., Degiacomi, C. G., Mekarnia, D. & Geballe, T. R. 1996, *ApJ*, 463, 336
- Bieging, John H. & Tafalla, Mario 1993, *AJ*, 105, 576
- Brunish, W. M. & Truran, J. W. 1982, *ApJ*, 256, 247
- Danchi, W. C., Bester, M., Degiacomi, C. G., Greenhill, L. J. & Townes, C. H. 1994, *AJ*, 107, 1469
- Dyck, H. M., Zuckerman, B., Leinert, Ch. & Beckwith, S. 1984, *ApJ*, 287, 801
- Glassgold, A. E. 1998, *IAU Symposia*, 191, 337
- Groenewegen, M.A.T. 1997, *A&A*, 317, 503
- Hale, David D. S., et al. 1997, *ApJ*, 490, 407
- Hale, D. D. S., et al. 2000, *ApJ*, 537, 998
- Haniff, C. A. & Buscher, D. F. 1998, *A&A*, 334, L5
- Herbig, G. H. & Zappala, R. R. 1970, *ApJ*, 162, L15

- Herbig, G. H. 1972, ApJ, 172, 375
- Ivezic, Z. & Elitzur, M. 1996, MNRAS, 279, 1019
- Kastner, J. H. & Weintraub, D. A. 1998, AJ, 115, 1592
- Knapp, G. R., Phillips, T. G., Leighton, R. B., Lo, K. Y., Wannier, P. G., Wootten, H. A. & Huggins, P. J. 1982, ApJ, 252, 616
- Lada, C. J. & Reid, M. J. 1978, ApJ, 219, 95
- Lipman, E. A. 1998, University of California at Berkeley, PhD Dissertation
- Lopez, B., et al. 1997, ApJ, 488, 807
- Maihara, T., Noguchi, K., Oishi, M., Okuda, H. & Sato, S. 1976, Nature, 259, 465
- Marvel, K. B. 1996, New Mexico State University, Ph.D. Dissertation
- Mathis, J. S., Rumpl, W. & Nordsieck, K. H. 1977, ApJ, 217, 425
- McCarthy, D. W., Jr. 1979, IAU Colloq. 50: High Angular Resolution Stellar Interferometry, 18
- Monnier, J. D., et al. 1997, ApJ, 481, 420
- Monnier, J. D., Geballe, T. R. & Danchi, W. C. 1998, ApJ, 502, 833
- Monnier, J. D. 1999, University of California at Berkeley, PhD Dissertation
- Monnier, J. D., Tuthill, P. G., Lopez, B., Cruzalebes, P., Danchi, W. C. & Haniff, C. A. 1999a, ApJ, 512, 351
- Monnier, J. D., Geballe, T. R. & Danchi, W. C. 1999b, ApJ, 521, 261
- Monnier, J. D., Danchi, W. C., Hale, D. S., Tuthill, P. G., & Townes, C. H. 2000, ApJ, in press
- Neugebauer, G. & Leighton, R. B. 1969, *Two micron sky survey : A preliminary Catalogue* (NASA SP-3047 [Washington, D.C.: Government Printing Office])
- Ossenkopf, V., Henning, Th. & Mathis, J. S. 1992, A&A, 261, 567
- Richards, A. M. S., Yates, J. A. & Cohen, R. J. 1998, MNRAS, 299, 319
- Ridgway, Stephen & Keady, John J. 1988, ApJ, 326, 843
- Rouleau, Francois & Martin, P. G. 1991, ApJ, 377, 526
- Le Sidaner, P. & Le Bertre, T. 1996, A&A, 314, 896
- Sahai, R. 1998, IAU Symposia, 191, 524P

- Skinner, C. J., Meixner, M. & Bobrowsky, M. 1998, MNRAS, 300, L29
- Smith, N., Humphreys, R. M., Krautter, J., Gehrz, R. D., Davidson, K., Jones, T. J. & Hubrig, S. 1999, American Astronomical Society Meeting, 194, 1306
- Toombs, R. I., Becklin, E. E., Frogel, J. A., Law, S. K., Porter, F. C. & Westphal, J. A. 1972, ApJ, 173, L71
- Toon, O. B., & Ackerman, T. P. 1981, Appl. Opt., 20, 3657
- Tuthill, P. G., Monnier, J. D., & Danchi, W. C. 1998, IAU Symposia, 191, 331
- Tuthill, P. G., Monnier, J. D., Danchi, W. C., & Lopez, B. 2000, ApJ, in press
- Weigelt, G., Balega, Y., Bloeker, T., Fleischer, A. J., Osterbart, R. & Winters, J. M. 1998, A&A, 333, L51
- Wolfire, Mark G. & Cassinelli, Joseph P. 1986, ApJ, 310, 207
- Worley, Charles E. 1972, ApJ, 175, L93

Table 5. VY CMa Model Parameters for Uniform Outflow Fit (November 1998 data)

Parameter	Value	Comments
Distance (pc)	1500	From Lada & Reid (1978)
T_{eff} (K)	2700	From Monnier <i>et al.</i> (1999a)
Stellar Radius (mas)	10.0	
Luminosity (L_{\odot})	5×10^5	Chosen to fit mid-IR spectrum
Dust Type	Silicates	From Ossenkopf, Henning, & Mathis (1992)
Dust Size Distribution	$n \propto a^{-3.5}$	From Mathis, Rumpl, & Nordsieck (1977)
R_{dust} (mas)	50	Dust inner radius, Chosen to fit mid-IR visibility
τ at $11.15\mu\text{m}$	2.41	Optical depth, Chosen to fit mid-IR spectral shape
Effective Primary Beamwidth (")	3.0	

Table 6. VY CMa Visibility Data from 1997 October 20 ($\lambda=11.15 \mu\text{m}$)

Spatial Frequency (10^5 rad^{-1})	Position Angle ($^\circ$)	Visibility	Visibility Uncertainty
2.7	330	0.247	0.044
3.1	320	0.242	0.021
3.5	314	0.204	0.031
3.9	310	0.192	0.027
4.3	306	0.168	0.016
4.7	304	0.135	0.015
5.1	301	0.098	0.020
5.8	299	0.077	0.012
6.4	297	0.078	0.010
6.8	296	0.073	0.010
7.2	296	0.063	0.011
7.7	295	0.053	0.010
8.1	295	0.035	0.009
8.5	295	0.029	0.013
8.8	294	0.046	0.011
9.2	294	0.039	0.011
9.7	294	0.024	0.016